Chapter 14
An Investigation of Nonlinear Solution Techniques for SSM-Reduced Mechanical Systems

Tiago S. Martins, F. Trainotti, L. Kreuzer, and D. J. Rixen

Abstract The parametrization method for invariant manifold reduction, has led to significant advancements in simplifying high-dimensional model reduction via direct computation of reduced dynamics in physical coordinates. Despite these advances, solving reduced systems requires efficient numerical methods. This paper investigates the effectiveness of three solvers—harmonic balance, orthogonal collocation, and shooting—on periodic orbit analysis within reduced-order models. Harmonic balance demonstrated a balance between computational speed and accuracy but was impacted by higher harmonic truncation. Orthogonal collocation, the most efficient for moderate time resolutions, required finer time discretization but scaled well with increasing complexity. Shooting, while initially slower, scaled effectively at higher resolutions but was sensitive to tolerance settings. The comparative analysis provides critical insights into the solvers' performance, offering practical guidance for nonlinear mechanical system analysis.

Keywords spectral submanifolds · reduced-order models · harmonic balance · orthogonal collocation · shooting method

Introduction

The parametrization method, first introduced by Cabré *et al.* [1–3], and later reformulated for engineering applications by Haro *et al.* [4], marked a major advancement in the reduction to invariant manifolds, unifying various approaches under a single framework. Previous methods [5] focused either on invariant manifold computations or relied on normal form theory [6]. The direct parametrization method, shows that both approaches can be derived from the invariance equation, solvable through graph or normal-form styles.

In [7], the parametrization method was adapted to vibratory systems addressing dissipation, while also providing existence and uniqueness theorems for invariant manifolds defined as spectral submanifolds (SSMs), leading to automated reduction methods [8] for two-dimensional manifolds with damping and arbitrary polynomial nonlinearities.

Subsequent advances [9] overcame the limitation of needing to express equations of motion in the modal basis, impractical for large finite element models, by enabling direct computations in physical coordinates. For mechanical systems, normal form-based methods and SSM approaches were developed [10–12] to express reduced dynamics in physical coordinates, incorporating damping and providing high-order automated approximations. These developments were made accessible through `SSMtool 2.0` [13], which automates the computation of high-order SSM approximations.

Futher on this topic, Opreni *et al.* [14] included additional non-autonomous terms for model order reduction in forced-damped mechanical structures with geometric nonlinearities, enabling the prediction of phenomena such as parametric excitation and isolated solutions. Li *et al.* [15] introduced a rigorous method for creating reduced-order models (ROMs) considering configuration constraints. Martin *et al.* [16] presented a direct parametrization method for reducing geometrically nonlinear rotating structures, with a focus on capturing the hardening/softening transition and interpolating ROMs. Axås *et al.* [17] established that the eigenvectors of delay-embedded systems are determined by their eigenvalues, allowing for preemptive identification of multimodal SSMs and their nonlinear interactions. Haller *et al.* [18] expanded the class of SSMs to include mixed stability types and fractional powers, enhancing low-dimensional polynomial models for nonlinear dynamics. Thurnher *et al.* [19] developed multi-index expressions for nonautonomous terms, facilitating resonance tongue extraction and steady-state response formulation in parametrically excited systems. Li *et al.* [20] presented an efficient

Tiago S. Martins · F. Trainotti · L. Kreuzer · D. J. Rixen
Technical University of Munich, Chair of Applied Mechanics, TUM School of Engineering and Design, Department of Mechanical Engineering. Boltzmannstr. 15 85748 Garching, Germany
e-mail: tiago.martins@tum.de; francesco.trainotti@tum.de; leo.kreuzer@tum.de; rixen@tum.de

Ludovic Renson et al. (eds.), *Nonlinear Structures & Systems, Vol. 1*, Conference Proceedings
of the Society for Experimental Mechanics Series, https://doi.org/10.13052/97887-438-0146-7_14

method for computing forced response surfaces in nonlinear systems, utilizing SSMs for ROMs and multidimensional manifold continuation to extract key features. Haller and Kaundinya [21] derived asymptotic expansions for weakly forced systems, providing techniques for persistent, normally hyperbolic SSMs under varying forces. Cenedese *et al.* [22] presented a data-driven approach to construct SSM-reduced models from finite element simulations, achieving accurate predictions for forced responses. Vizzaccaro *et al.* [23] introduced a novel method to handle superharmonic resonances through expanded parametrizing coordinates. Bettini *et al.* [24] proposed a technique for sparse, nonlinear models on slow attracting spectral submanifolds applicable to various system types. And most recently, Grolet *et al.* [25] formulated a method to transform differential-algebraic equations with non-polynomial nonlinearities into polynomial systems, addressing geometric exactness in finite element structures.

Despite advancements in the computational frameworks presented in these papers, robust solvers are still required to effectively navigate the resultant reduced systems. This paper builds upon previous reduction methods by focusing on the identification of periodic orbits within these reduced systems. The discussion is supported by an example of a ROM of an arch beam generated by `MORFE2.0` [23] and compares three prominent numerical techniques—harmonic balance, orthogonal collocation, and shooting—on their effectiveness in solving the corresponding reduced-order dynamics.

The harmonic balance [26] method analyzes periodic solutions by transforming nonlinear problems into the frequency domain. Orthogonal collocation [27], is based on polynomial approximations and collocation points. Lastly, the shooting method [28] solves the periodic boundary value problems through iterative adjustments of initial conditions. MatCont [29] was used for orthogonal collocation and the other methods were purposely coded for this work.

This study evaluates the three solver methods in the context of reduced-order models to provide valuable insights into the dynamics of nonlinear mechanical systems and offer practical guidance for engineers and researchers. However, it does not exhaustively explore variations and alternatives in nonlinear solver techniques; it only employs the tangent predictor with pseudo-arclength continuation, the alternating frequency-time scheme for harmonic balance, orthogonal collocation at gaussian points, and single shooting.

The analysis begins with the full order dynamical system described by the following first-order autonomous ODE which can encompass a general class of physical systems, including second-order mechanical systems casted to first-order.

$$\dot{\mathbf{x}} = \mathbf{f}(\mathbf{x})\,. \tag{1}$$

Direct Parameterization of Invariant Manifolds

The following is a summary of the method described in [13, 30]. The goal is to generate a reduced dynamical system $\dot{\mathbf{q}} = \mathbf{g}(\mathbf{q})$, i.e. of lower dimension, whose orbits approximate solutions of the full system, close to a stable equilibrium, when mapped through another constructed function, called the manifold parameterization, namely $\mathbf{x} = \mathbf{W}(\mathbf{q})$.

The assumption is that the full dynamics $\mathbf{f}$, the reduced dynamics $\mathbf{g}$ and the manifold parameterization $\mathbf{W}$ are power series. Given $n, m \in \mathbb{N}$ with $m < n$, an open set $U \in \mathbb{R}^n$ containing the origin and an open set $V \in \mathbb{C}^m$ containing the origin, define the functions[1]

$$\begin{aligned}
&\mathbf{f} : U \to \mathbb{R}^n && \mathbf{W} : V \to U && \mathbf{g} : V \to \mathbb{C}^m \\
&\quad \mathbf{x} \mapsto \mathbf{f}(\mathbf{x}) = \sum_{\kappa \in \mathbb{N}} \mathbf{f}_\kappa \mathbf{x}^{\otimes \kappa} && \quad \mathbf{q} \mapsto \mathbf{W}(\mathbf{q}) = \sum_{\kappa \in \mathbb{N}} \mathbf{W}_\kappa \mathbf{q}^{\otimes \kappa} && \quad \mathbf{q} \mapsto \mathbf{g}(\mathbf{q}) = \sum_{\kappa \in \mathbb{N}} \mathbf{g}_\kappa \mathbf{q}^{\otimes \kappa}\,.
\end{aligned}$$

Without loss of generality, it is clear that an equilibrium is placed at the origin, as $\mathbf{f}(\mathbf{0}) = \mathbf{0}$. Hence, via direct substitution, one has

$$\frac{\mathrm{d}\mathbf{W}}{\mathrm{d}\mathbf{q}}(\mathbf{q})\,\mathbf{g}(\mathbf{q}) \approx \mathbf{f}(\mathbf{W}(\mathbf{q})) \iff \left(\sum_{\kappa \in \mathbb{N}} \mathbf{W}_\kappa \frac{\mathrm{d}}{\mathrm{d}\mathbf{q}} \mathbf{q}^{\otimes \kappa}\right)\left(\sum_{\sigma \in \mathbb{N}} \mathbf{g}_\sigma \mathbf{q}^{\otimes \sigma}\right) \approx \sum_{\sigma \in \mathbb{N}} \mathbf{f}_\sigma \left(\sum_{\kappa \in \mathbb{N}} \mathbf{W}_\kappa \mathbf{q}^{\otimes \kappa}\right)^{\otimes \sigma}\,.$$

The method matches all the polynomial terms up to some chosen degree, such as to accumulate all the error in higher order terms, as with the idea that underlies Taylor expansions. Therefore, equating the coefficients of order γ yields

$$\sum_{\kappa=1}^{\gamma} \mathbf{W}_\kappa \boldsymbol{\Gamma}_{\gamma,\kappa} = \sum_{\kappa=1}^{\gamma} \mathbf{f}_\kappa \boldsymbol{\Xi}_{\gamma,\kappa}\,, \tag{2}$$

[1] The Kronecker power denotes the repeated Kronecker product such that: $\mathbf{x}^{\otimes 0} = [1]$, the uni-dimensional identity matrix; and $\mathbf{x}^{\otimes \kappa} = \underbrace{\mathbf{x} \otimes \mathbf{x} \otimes \cdots \otimes \mathbf{x}}_{\kappa \text{ times}}$ for $\kappa \in \mathbb{N}$.

where $\mathbf{\Gamma}_{\gamma,\kappa}$ and $\mathbf{\Xi}_{\gamma,\kappa}$ can be defined by the following recurrence relations

$$\mathbf{\Gamma}_{\gamma,1} = \mathbf{g}_\gamma \qquad \mathbf{\Gamma}_{\gamma+1,\kappa+1} = \mathbf{I}_m \otimes \mathbf{\Gamma}_{\gamma,\kappa} + \mathbf{g}_{\gamma-\kappa+1} \otimes \mathbf{I}_{m^\kappa},$$

$$\mathbf{\Xi}_{\gamma,1} = \mathbf{W}_\gamma \qquad \mathbf{\Xi}_{\gamma,\kappa+1} = \sum_{\sigma=\kappa}^{\gamma-1} \mathbf{W}_{\gamma-\sigma} \otimes \mathbf{\Xi}_{\sigma,\kappa}.$$

Here, $\mathbf{\Gamma}_{\gamma,\kappa}$ is a $m^\kappa \times m^\gamma$ complex matrix whose entries are sums of κ elements of $\mathbf{g}_{\gamma-\kappa+1}$. Additionally, $\mathbf{\Xi}_{\gamma,\kappa}$ is a $n^\kappa \times m^\gamma$ complex matrix whose entries are sums of products involving elements of $\mathbf{W}_1$, $\mathbf{W}_2$, ... and $\mathbf{W}_{\gamma-\kappa+1}$. In particular, it can be seen that $\mathbf{\Xi}_{\gamma,\gamma} = \mathbf{W}_1^{\otimes\gamma}$.

In the literature, $\mathbf{\Gamma}_{\gamma,\kappa}$ and $\mathbf{\Xi}_{\gamma,\kappa}$ are defined with closed form expressions. However, here they are stated via recurrence to suggest an efficient computation algorithm, as is the topic of this work.

Now, regarding the goal of constructing the reduced dynamics $\mathbf{g}$ and the manifold parameterization $\mathbf{W}$, one must solve equation (2) for $\mathbf{W}_\gamma$ and $\mathbf{g}_\gamma$ with γ ranging from 1 up to the desired expansion order, $\gamma_{\max}$. At its simplest case, for order $\gamma = 1$, equation (2) becomes

$$\mathbf{W}_1 \mathbf{g}_1 = \mathbf{f}_1 \mathbf{W}_1, \tag{3}$$

which can be made an eigenvalue problem by imposing $\mathbf{g}_1$ to be diagonal. In that case, $\mathbf{\Gamma}_{\gamma,\gamma}$ is a diagonal matrix comprised of all the possible sums of γ eigenvalues of $\mathbf{g}_1$.

Given $\gamma \geq 2$, by collecting the terms of equation (2) that depend on $\mathbf{W}_\gamma$ and $\mathbf{g}_\gamma$, one defines

$$\mathcal{L}_\gamma(\mathbf{W}_\gamma, \mathbf{g}_\gamma) = \mathbf{W}_\gamma \mathbf{\Gamma}_{\gamma,\gamma} - \mathbf{f}_1 \mathbf{W}_\gamma + \mathbf{W}_1 \mathbf{g}_\gamma,$$

where $\mathcal{L}_\gamma$ is a linear map between complex vector spaces of dimension $nm^\gamma + m^{\gamma+1}$ and nm^γ. Subsequently, accumulating all the remaining terms of (2), one constructs

$$\mathbf{B}_\gamma = \sum_{\kappa=2}^{\gamma} \mathbf{f}_\kappa \mathbf{\Xi}_{\gamma,\kappa} - \sum_{\kappa=2}^{\gamma-1} \mathbf{W}_\kappa \mathbf{\Gamma}_{\gamma,\kappa},$$

which only depends on the coefficients of $\mathbf{W}$ and $\mathbf{g}$ up to order $\gamma - 1$, and on the coefficients of $\mathbf{f}$ up to order γ. Finally, the equivalent homological equation of order $\gamma \geq 2$ becomes

$$\mathcal{L}_\gamma(\mathbf{W}_\gamma, \mathbf{g}_\gamma) = \mathbf{B}_\gamma. \tag{4}$$

Equations (3) and (4) can be used to define a procedure for building the manifold parameterization $\mathbf{W}$ and reduced dynamics $\mathbf{g}$. Namely, non-trivial solutions of (3) produce $\mathbf{W}_1$ and $\mathbf{g}_1$, which are used to construct the linear equation (4) at order 2, that is then solved for $\mathbf{W}_2$ and $\mathbf{g}_2$. All the previous solutions are processed to build the order 3 equation, which can be linearly solved for $\mathbf{W}_3$ and $\mathbf{g}_3$, that can again be recycled to compute order 4, and so forth.

Whenever there are nontrivial intersections between the eigenspace of $\mathbf{\Gamma}_{\gamma,\gamma}$ and the eigenspace of $\mathbf{f}_1$, there are resonance phenomena; nonlinear if $\gamma > 1$. If that intersection is in the eigenspace of $\mathbf{\Gamma}_{1,1} = \mathbf{g}_1$, the span of the m linear modes, there is inner resonance, since the movement of the nonlinear resonance is spanned by the linear modes $\mathbf{W}_1$. Conversely, there is outer resonance which in practice means that equation (4) might be unsolvable [13].

Because the dimension of the codomain of $\mathcal{L}_\gamma$ is smaller than that of its domain, there may be multiple solutions to equation (4), and it is common to parameterize the solution space [14]. The normal-form style of parameterization starts by determining the image of $\mathcal{L}_\gamma(\cdot, \mathbf{0})$, by detecting nonlinear resonances, then solves for $\mathbf{W}_\gamma$ with fixed $\mathbf{g}_\gamma = \mathbf{0}$ by projecting $\mathbf{B}_\gamma$ on said image, and solves for $\mathbf{g}_\gamma$ with fixed $\mathbf{W}_\gamma = \mathbf{0}$ on the complementary subspace. The graph style of parameterization is similar but assumes that all possible nonlinear resonances occur.

Additionally, the fact that the initial problem is real can be leveraged to improve computational efficiency. Specifically, this allows for the construction of $\mathbf{g}$ and $\mathbf{W}$ as mappings between real spaces of dimension m, halving the *real dimension* of the original definition. Henceforth, this works assumes that realification was performed.

Practical issues

There are many large matrices involved in this procedure, therefore it is advised to explore sparsity and symmetry, use smart memory allocation and properly scalable algorithms to combat computational limitations. It can be seen that the size of the

matrices increases exponentially with the polynomial degree and polynomially with the number of degrees of freedom as $O(n^\gamma m^\gamma)$. The number of matrices increases factorially since there are $\binom{\gamma+m-1}{m-1}$ monomials of degree γ.

Furthermore, it is important to understand that this is a local method that relies on polynomial expansions. Therefore one must be careful when applying it to nonlinear problems and generating results far from the equilibrium.

External forcing terms are simulated as stable solutions of well chosen ODEs: $\dot{\mathbf{x}}_\mathrm{F} = \mathbf{f}_\mathrm{F}(\mathbf{x}_\mathrm{F})$. The internal dynamics then depend on the internal state and the state of the external forcing: $\dot{\mathbf{x}}_\mathrm{S} = \mathbf{f}_\mathrm{S}(\mathbf{x}_\mathrm{S}, \mathbf{x}_\mathrm{F})$. For example, regarding sinusoidal forcing, for any $\overline{\beta}, \omega, \phi \in \mathbb{R}$

$$\begin{cases} \beta_\mathrm{F}(t) = \overline{\beta} \\ x_\mathrm{F}(t) = \beta_\mathrm{F}(t)\cos(\omega t + \phi) \\ y_\mathrm{F}(t) = \beta_\mathrm{F}(t)\sin(\omega t + \phi) \end{cases} \quad \text{is a stable solution of} \quad \begin{cases} \dot{\beta}_\mathrm{F} = 0 \\ \dot{x}_1 = -\omega y_\mathrm{F} - x_\mathrm{F}\,(x_\mathrm{F}^2 + y_\mathrm{F}^2 - \beta_\mathrm{F}^2) \\ \dot{y}_\mathrm{F} = +\omega x_\mathrm{F} - y_\mathrm{F}\,(x_\mathrm{F}^2 + y_\mathrm{F}^2 - \beta_\mathrm{F}^2) \end{cases} . \tag{5}$$

In practice, this involves appending extra equations to describe the forcing, ensuring $\mathbf{f}_\mathrm{F}(\mathbf{0}) = \mathbf{0}$ to retain the equilibrium at the origin and guaranteeing that the forcing stays close to the equilibrium state: in the example above, by having a small absolute value for $\overline{\beta}$. On this matter, having forcing of multiple frequencies has been discussed [19], but it requires more complex theory and implementation. In the case of `MORFE2.0` [23], that feature was yet unavailable.

Moreover, the choice of style significantly impacts results and efficiency: the graph style is slower than the normal-form style, in general, but more useful in the context of center manifold computation, while the normal style provides simpler reduced dynamics and uniquely describes manifold folding [14]. Also, to avoid outer resonance, all the modes of the full order model, that (nonlinearly) resonate with the master modes up to order γ_max, must be included from the start.

Nonlinear Solvers for Computing Periodic Solutions

Harmonic Balance via Alternating Frequency-Time

One first assumes that $\mathbf{q}(t)$ is a Fourier series, which already guarantees periodicity, restricted to the harmonics in a previously chosen finite set of non-negative integers $\mathcal{H}$:

$$\mathbf{q}(t) = \mathrm{Re} \sum_{h \in \mathcal{H}} \mathbf{Q}_h \exp(\mathrm{i}h\omega t)\,.$$

This allows expressing $\dot{\mathbf{q}}(t)$ and $\mathbf{g}(\mathbf{q}(t))$ as Fourier series with coefficients $\mathrm{i}h\omega\mathbf{Q}_h$ and $\mathbf{G}_h$ for harmonic $h \in \mathcal{H}$, respectively. Via the alternating frequency-time scheme, one has

$$\mathbf{G}_h = \mathrm{rDFT}(\{\mathbf{g}(\mathbf{q}_k)\}_{k=1}^N)_h \quad \text{with} \quad \mathbf{q}_k = \mathrm{irDFT}(\{\mathbf{Q}_h\}_{h\in\mathcal{H}})_k\,,$$

where rDFT and irDFT are the real discrete Fourier transform and its inverse. The computation of $\mathbf{G}_h$ can be made exact for polynomial nonlinearities (the case of this work) by having enough time samples: $N > (\gamma_\mathrm{max} + 1)\, h_\mathrm{max}$, as in [31]. In practice, the computation of these functions is done with divide and conquer algorithms like the fast Fourier transform. This way, the ODE of the reduced dynamics, $\dot{\mathbf{q}} = \mathbf{g}(\mathbf{q})$, is transformed into the family of algebraic equations

$$\mathrm{i}r\omega\mathbf{Q}_r = \mathbf{G}_r(\{\mathbf{Q}_h\}_{h\in\mathcal{H}}) \quad \text{with} \quad r \in \mathcal{H}\,.$$

It is possible to write an equivalent set of twice as many equations[2] using only real numbers, by separating the real and imaginary parts of all the quantities involved, resulting in $2m|\mathcal{H}|$ real polynomial equations of degree $\leq \max(\gamma_\mathrm{max}, 2)$ with $2m|\mathcal{H}|+1$ real unknowns, including ω.

The irDFT naturally computes $N = 2h_\mathrm{max}$ time domain samples, given the set of non-negative harmonics $\mathcal{H}$ and $h_\mathrm{max} = \max\mathcal{H}$, which defines the resolution of the harmonic balance method.

Orthogonal Collocation

The T-normalized time interval $[0,1]$ is divided into z test intervals with variable[3] duration, forming the coarse mesh: $0 = \tau_0 < \tau_1 < \cdots < \tau_z = 1$. Each interval is further subdivided into $c+1 \in \mathbb{N}$ subintervals, via c Gaussian collocation points[4],

[2] The equation of harmonic zero is already a real equation. When $0 \in \mathcal{H}$, one gets $2m|\mathcal{H}| - 1$ real polynomial equations with $2m|\mathcal{H}|$ real unknowns, including ω.

[3] In MatCont [29], the coarse mesh is adapted after a certain amount of solution points.

[4] In MatCont [29], the collocation points are the roots of the c-th Legendre polynomial, shifted and scaled.

forming the fine mesh $\{\tau_{\sigma,\kappa}\}$ such that

$$\tau_\sigma < \tau_{\sigma,1} < \cdots < \tau_{\sigma,c} < \tau_{\sigma+1} \quad \text{with} \quad \sigma \in \{0,\dots,z-1\}\,.$$

The method assumes that the limit cycle is approximated by a continuous piecewise polynomial in each of the coarse mesh intervals:

$$\mathbf{q}(t=\tau/\omega) = \mathbf{p}(\tau) = \mathbf{p}_\sigma(\tau)\,, \quad \tau \in [\tau_\sigma, \tau_{\sigma+1}] \quad \text{with} \quad \mathbf{p}_\sigma(\tau_{\sigma,c}) = \mathbf{p}_{\sigma+1}(\tau_{\sigma,c})\,,$$

where $\mathbf{p}_\sigma$ is the degree-c orthogonal polynomial relevant to the σ-th coarse mesh interval. The second condition ensures continuity at the coarse mesh, and imposing periodicity yields $\mathbf{p}_\sigma(\tau_0) = \mathbf{p}_{z-1}(\tau_z)$. Finally, the method aims to ensure that the ansatz complies with the dynamics at each of the $N = cz$ fine mesh points, expressly

$$\omega\mathbf{p}'(\tau_{\sigma,\kappa}) = 2\pi\,\mathbf{g}(\mathbf{p}(\tau_{\sigma,\kappa})) \quad \text{with} \quad \sigma \in \{0,\dots,z-1\} \quad \text{and} \quad \kappa \in \{1,\dots,c\}\,.$$

For a system of dimension m, at each of the z coarse mesh intervals, the local polynomial is defined by $(c+1)m$ coefficients, which yields a total of $(c+1)zm+1$ unknowns accounting for ω. Per coarse mesh interval, there are cm collocation constraints for the dynamics and m continuity (and periodicity) constraints, totaling $(c+1)zm$ polynomial equations of degree $\leq \max(\gamma_{\max}, 2)$.

On this note, harmonic balance can also be viewed as a frequency domain orthogonal collocation method, where complex exponentials form an orthonormal basis, and the residue must vanish at specific harmonics, effectively "collocating" or enforcing the system dynamics at key frequencies, rather than in the time domain.

Single Shooting

Shooting converts the periodic boundary-value problem into an initial-value problem. In this approach, an initial guess for the system's state is made, and the system's equations of motion are integrated over time to compute the state at the end of the period. For a given initial condition $\mathbf{q}_0 = \mathbf{q}(0)$, the flow $\boldsymbol{\varphi}(\mathbf{q}_0, 1)$ maps the initial state to the final state after a time period T by solving the time-normalized differential equations. Namely, $\boldsymbol{\varphi}(\mathbf{q}_0, \cdot) : \mathbb{R} \to \mathbb{R}^m$ solves

$$\boldsymbol{\varphi}'(\mathbf{q}_0, \tau) = T\,\mathbf{g}(\boldsymbol{\varphi}(\mathbf{q}_0, \tau)) \quad \text{and} \quad \boldsymbol{\varphi}(\mathbf{q}_0, 0) = \mathbf{q}_0\,,$$

where the derivative is with respect to $\tau = t/T$. Moreover, periodicity is stated through the constraint $\boldsymbol{\varphi}(\mathbf{q}_0, 1) = \mathbf{q}_0$, with m equations and $m+1$ unknowns, including T.

The flow is approximated via a direct (transient) time integration method. This work uses the fourth order Runge-Kutta method, chosen for its accuracy and simplicity, with N evenly spaced time steps. At each time increment, the next state becomes a weighted average of four state estimations which are computed by recursively evaluating the time-normalized dynamics $T\mathbf{g}(\cdot)$, which has degree $\gamma_{\max}+1$ on $(\mathbf{q}_0, T)$. Hence, accounting for the four levels of recursion at each of the N time increments, $\boldsymbol{\varphi}(\mathbf{q}_0, T)$ can be interpreted as a polynomial of degree $4N[\gamma_{\max}+1]$.

Numerical Continuation

In all the aforementioned methods, the problem of finding periodic solutions to the reduced dynamics can be reformulated as solving an algebraic equation, $\mathbf{R}(\mathbf{X}) = \mathbf{0}$, where $\mathbf{X}$ is the vector of unknowns (including the frequency) and $\mathbf{R}$ defines the constraints: Fourier coefficients with frequency collocation constraints for harmonic balance, polynomial coefficients with collocation and continuity constraints for orthogonal collocation, and the initial state with the periodicity constraint for shooting. Predictor corrector numerical continuation aims to find a sequence of solution points by using the last solution $\mathbf{X}_{\text{last}}$ and executing a predictor procedure to estimate a new solution $\mathbf{X}_0$ which is then iteratively refined by a corrector procedure. In this work, the tangent prediction method, defined as follows, was used:

$$\mathbf{X}_0 = \mathbf{X}_{\text{last}} + s\mathbf{V} \qquad \text{with } \mathbf{V} \text{ such that} \qquad \left.\frac{\mathrm{d}\mathbf{R}}{\mathrm{d}\mathbf{X}}\right|_{\text{last}} \mathbf{V} = \mathbf{0}\,, \qquad \mathbf{V}_{\text{ref}}^{\mathrm{T}}\mathbf{V} > 0\,, \qquad \|\mathbf{V}\| = 1\,,$$

where $s > 0$ is the step length and $\mathbf{V}_{\text{ref}}$ is a reference vector for the direction of the continuation, e.g. the secant through the last two solutions. The guess $\mathbf{X}_0$ is assumed to be close to the curve, hence it is used to initialize a Newton based corrector procedure to find a new solution. Since the standard Newton iterations can only be applied to systems with the same number of equations as unknowns, one extra scalar condition is appended: the pseudo-arclength parameterization, $p(\mathbf{X}) = \mathbf{V}^{\mathrm{T}}(\mathbf{X} - \mathbf{X}_0)$. Equating it to zero limits the solution to a hyperplane orthogonal to the predictor vector $\mathbf{V}$ and passing through the guess $\mathbf{X}_0$. Finally, the step length s is adjusted according to the number of iterations in the previous corrector step, in an inverse manner, to place the next guess in the fast convergence region of the Newton corrector.

Application and Discussion of Results

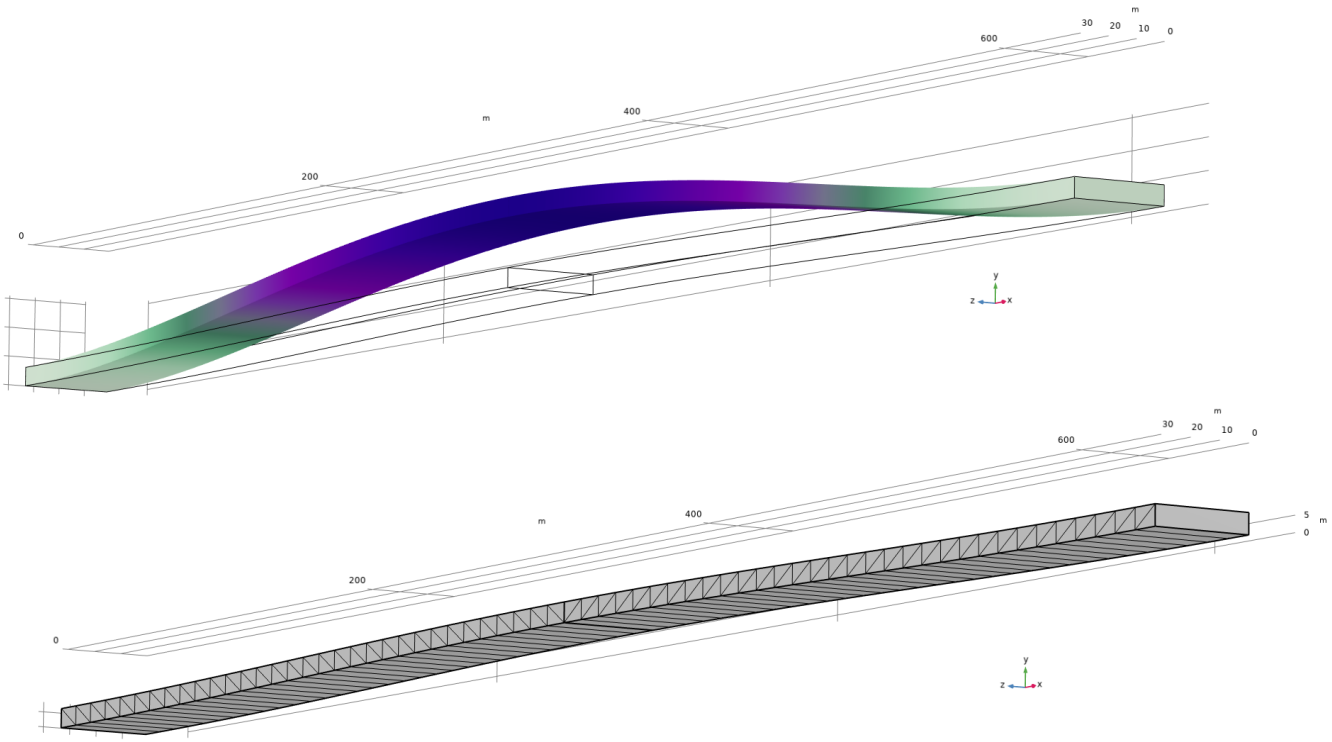

Fig. 1 Full-order finite element model of the clamped-clamped arch-beam. Geometry and mesh on top. Shape of the first linear eigenmode, below. Generated in COMSOL Multiphysics 6.2 [32].

The analysis begins with a full-order finite element model (of second-order elements) of the clamped-clamped arch-beam depicted in figure 1, which does not have preload and is anticipated to exhibit geometric nonlinear behavior. Figure 1 also illustrates the shape of the first linear mode, characterized by an eigenfrequency of $\omega_1 = 1.03308$. In `MORFE2.0` [23], the external force is represented as a small modal excitation of mode 1, with light mass-proportional damping introduced to achieve a damping ratio of 0.1%. The reduction settings are defined as follows: the maximum expansion order is set to $\gamma_{\max} = 7$; one master mode was utilized from the ten computed to identify outer resonances; and the (complex) normal-form parameterization style was chosen.

For this study case, `MORFE2.0` [23] took[5] 110s to reduce the full order model of 2664 degrees of freedom into a ROM with just 2 normal coordinates. There are 2 additional decoupled forcing variables, like those in example (5), which can be directly substituted by sinusoidal functions.

The references in figure 2 were obtained by computing periodic solutions to the reduced dynamics, on the frequency range $\omega \in [0.7\omega_1, 1.3\omega_1]$, via harmonic balance, orthogonal collocation and shooting with a time-resolution of $N = 160$, residual tolerance of $\text{tol} = 10^{-9}$ and maximum allowed step length of $s_{\max} = 0.1$. Figures 3 and 4 were generated by running the solvers with varying parameters—time resolution, continuation step length and tolerance—while only including those that traced smooth frequency-response curves with proper resolution of the resonance. It is relevant to state that the "loop" intersections observed close to the resonance are an artifact of the projection of the frequency-response curves to a bidimensional plot, in fact the intersection corresponds to two different solutions.

Figure 3 cannot be directly used to rank method performance without discussion, as variations may arise from differences in software optimization and user expertise, and most importantly from the particularities of the methods themselves. For instance, figure 4 suggests that harmonic balance yields meaningful results with coarser time resolution, while shooting and especially orthogonal collocation require larger N to compute accurate frequency-response curves.

[5]The computer used in this work has an AMD Ryzen 9 7950X 16-Core Processor running at 4.50GHz and 128GB of RAM.

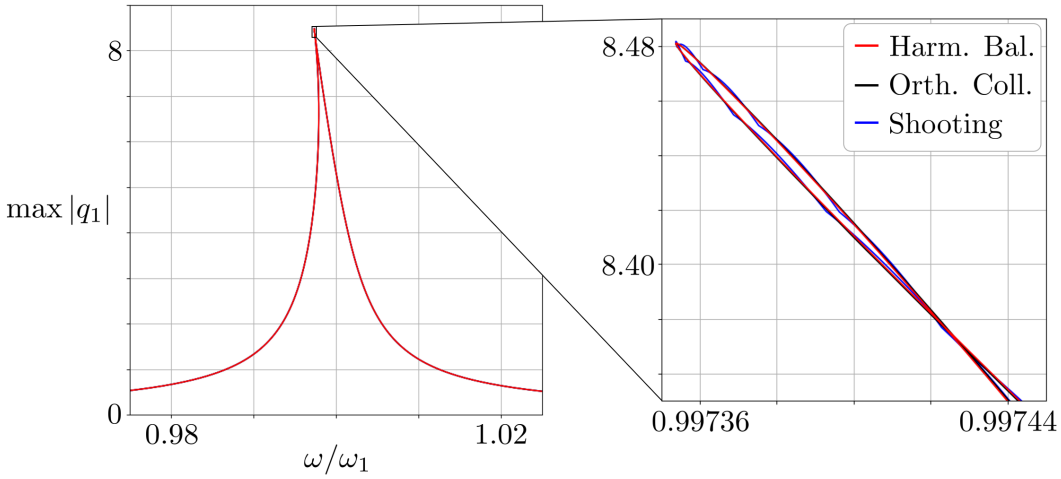

Fig. 2 Reference frequency-response curves of the SSM-reduced arch-beam computed using harmonic balance, orthogonal collocation and shooting with tolerance tol = 10^{-9}, maximum continuation step length $s_{\max} = 0.1$ and time resolution $N = 160$. The left plot is an amplification of the resonance region. The ratio between the frequency and the first linear eigenfrequency is ω/ω_1 and the maximum amplitude of first normal coordinate is $\max|q_1|$.

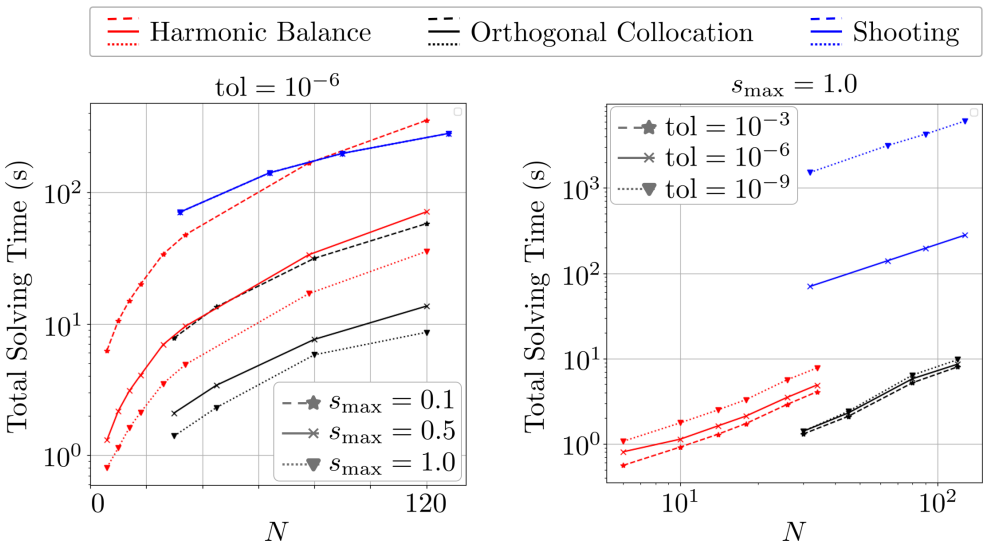

Fig. 3 Comparison of computation times for harmonic balance, orthogonal collocation and shooting regarding the construction of the frequency-response curve of the SSM-reduced arch beam. N indicates the time resolution, $s_{\max}$ is the maximum continuation step length and tol is the tolerance, whose meaning varies by method; the discussion section explains how to make the values comparable. On the left tol = 10^{-6} is fixed, and on the right $s_{\max} = 1.0$.

Harmonic Balance via Alternating Frequency-Time

Harmonic balance[6] achieves qualitatively accurate solutions with few harmonics (small $N = 2h_{\max}$) due to the Fourier series ansatz, which is optimized for finding periodic orbits and exhibits exponential convergence with truncation order $h_{\max}$, for smooth signals. When low truncation orders suffice to describe periodic time responses of low-dimensional smooth systems, the problem size and computation time are significantly reduced, leading to strong performance. On the other hand, including a large amount of harmonics significantly slows down the procedure due to the complexity of performing Newton iterations with larger matrices and the increased number of FFTs required.

[6] As a note, the set of harmonics $\mathcal{H}$ was optimized to include just odd harmonics, because the $\mathbf{g}$ of the system in question is an odd function and the forcing only excites the first harmonic.

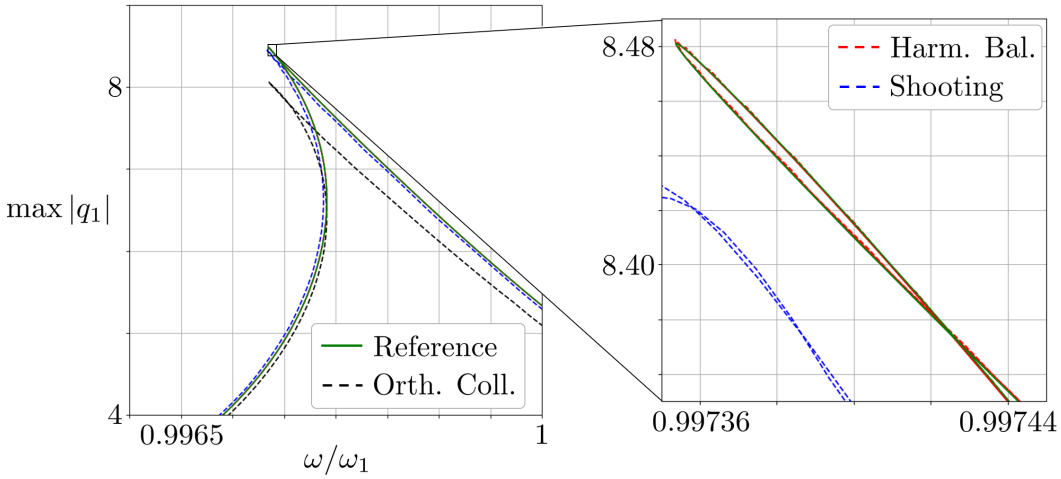

Fig. 4 Comparison to reference of frequency-response curves of the SSM-reduced arch-beam computed using harmonic balance ($N = 10$ and 0.93s), orthogonal collocation ($N = 30$ and 1.3s) and shooting ($N = 25$ and 21.2s) with the minimal parameters required for convergence. The left plot is an amplification of the resonance region. The ratio between the frequency and the first linear eigenfrequency is ω/ω_1 and the maximum amplitude of first normal coordinate is $\max|q_1|$.

Targeting a number of iterations of 0 (fully relying on the predictor) or 1 leads to impractically long computation times, particularly as the problem size increases. In contrast, setting a target of 2, 3, or 4 yields relatively consistent computation times, with slight improvements for larger values. Naturally, a larger maximum continuation step length significantly accelerates the procedure by enabling a coarser computation of regions of rapid convergence and (ideally) less intricate features. However, it is crucial to ensure that the average number of iterations is not excessively high, as this can lead to overly large step lengths resulting in low-resolution frequency-response curves.

Orthogonal Collocation

Orthogonal collocation proved to be the fastest method for the range $30 \leq N \leq 120$, benefiting from the analytical nature of the state $\mathbf{q}$, which allows the Lagrange polynomials to exhibit uniform exponential convergence.

Similar to harmonic balance, the methods involves $O(Nm)$ polynomial equations of degree $\gamma_{\max}$, where $N = cz$ is the time resolution and m is the dimension of the reduced dynamics. However, orthogonal collocation requires a finer time resolution than harmonic balance to achieve comparable accuracy, despite its computation time scaling more slowly with increasing N. As shown in figure 4, orthogonal collocation can fail to produce accurate results for N larger than of harmonic balance, while still able to converge in a comparable amount of time.

Remarkably, for fixed maximum step length, changing the tolerance had a very small effect on the speed of collocation, opposite to what happens with shooting.

Single Shooting

The residue in shooting, defined as the difference between final and initial states, $\mathbf{q}(T) - \mathbf{q}(0)$, is not directly comparable to residues in other methods, which relate to the "force" $\mathbf{g}(\mathbf{q})$. To ensure a fair comparison, the shooting solutions were post-processed to yield a corresponding residue magnitude of $\|\mathbf{g}(\mathbf{q}(T)) - \mathbf{g}(\mathbf{q}(0))\|$. Figure 3 illustrates that the shooting method is slower compared to the other two methods for lower time resolutions, and suggests that it might scale better for higher N.

Furthermore, no valid solutions were obtained for tol $= 10^{-3}$ and $s_{\max} \geq 0.1$, as the continuation procedure exhibited erratic behavior, including jumping along the solution curve, backtracking, and becoming trapped in loops of solutions. Instead, for tol $= 10^{-5}$, additional data points revealed times of $27.30, 54.32, 76.36, 108.26$ seconds for $N = 32, 64, 90, 128$, respectively. Shooting was the most sensitive to tol, with the computation time increasing approximately linearly with the number of time steps, for all cases.

The step lengths observed during the shooting runs were, on average, orders of magnitude smaller than the maximum allowed step lengths of 1.0, 0.5, and 0.1, indicating no practical benefit from increasing the step length within this range. Moreover, the optimal goal number of iterations was determined to be 1, as 0 resulted in impractically small step lengths and an excessive number of solution points, while 2 in unstable erratic behavior.

Shooting has to solve $O(m)$ polynomial equations of degree $O(N\gamma_{\max})$. While the number of equations is reduced, they are significantly more complex to manage. In particular, accurately approximating the flow through time integration is a challenging task.

Conclusion

Advancements in the parametrization method, particularly its adaptation to vibratory systems and the introduction of spectral submanifolds (SSMs), have greatly simplified the reduction of high-dimensional models. While the automated computation of reduced dynamics in physical coordinates marks significant progress, robust numerical solvers remain essential.

This study evaluated three solvers—harmonic balance, orthogonal collocation, and shooting—for periodic orbit analysis. Harmonic balance provided an effective trade-off between speed and accuracy but slowed with higher harmonics. Orthogonal collocation, the fastest for moderate resolutions, required finer time steps yet scaled well. Single shooting, while slower initially, scaled efficiently with increasing resolution but was highly sensitive to tolerance.

Acknowledgments The authors acknowledge Alessandra Vizzaccaro for her invaluable help regarding `MORFE2.0` [23].

Disclosure statement No potential conflict of interest is reported by the authors.

References

[1] Xavier Cabré, Ernest Fontich, and Rafael De la Llave. “The parameterization method for invariant manifolds I: manifolds associated to non-resonant subspaces”. In: *Indiana University mathematics journal* (2003), pp. 283–328.

[2] Xavier Cabré, Ernest Fontich, and Rafael De la Llave. “The parameterization method for invariant manifolds II: regularity with respect to parameters”. In: *Indiana University mathematics journal* (2003), pp. 329–360.

[3] Xavier Cabré, Ernest Fontich, and Rafael De La Llave. “The parameterization method for invariant manifolds III: overview and applications”. In: *Journal of Differential Equations* Vol. 218.No. 2 (2005), pp. 444–515.

[4] Alex Haro, Marta Canadell, Jordi-Lluis Figueras, Alejandro Luque, and Josep-Maria Mondelo. “The parameterization method for invariant manifolds”. In: *Applied mathematical sciences* Vol. 195 (2016).

[5] John Guckenheimer and Philip Holmes. *Nonlinear oscillations, dynamical systems, and bifurcations of vector fields*. Vol. 42. Springer Science & Business Media, 2013.

[6] Cyril Touzé, Olivier Thomas, and Antoine Chaigne. “Hardening/softening behaviour in non-linear oscillations of structural systems using non-linear normal modes”. In: *Journal of Sound and Vibration* Vol. 273.No. 1-2 (2004), pp. 77–101.

[7] George Haller and Sten Ponsioen. “Nonlinear normal modes and spectral submanifolds: existence, uniqueness and use in model reduction”. In: *Nonlinear dynamics* Vol. 86 (2016), pp. 1493–1534.

[8] Sten Ponsioen, Tiemo Pedergnana, and George Haller. “Automated computation of autonomous spectral submanifolds for nonlinear modal analysis”. In: *Journal of sound and Vibration* Vol. 420 (2018), pp. 269–295.

[9] Jorge Gonzalez, JD Mireles James, and Necibe Tuncer. “Finite element approximation of invariant manifolds by the parameterization method”. In: *Partial Differential Equations and Applications* Vol. 3.No. 6 (2022), p. 75.

[10] Alessandra Vizzaccaro, Yichang Shen, Loıc Salles, Jiří Blahoš, and Cyril Touzé. “Direct computation of nonlinear mapping via normal form for reduced-order models of finite element nonlinear structures”. In: *Computer Methods in Applied Mechanics and Engineering* Vol. 384 (2021), p. 113957.

[11] Yichang Shen, Alessandra Vizzaccaro, Nassim Kesmia, Ting Yu, Loıc Salles, Olivier Thomas, and Cyril Touzé. “Comparison of reduction methods for finite element geometrically nonlinear beam structures”. In: *Vibration* Vol. 4.No. 1 (2021), pp. 175–204.

[12] Andrea Opreni, Alessandra Vizzaccaro, Attilio Frangi, and Cyril Touzé. “Model order reduction based on direct normal form: application to large finite element MEMS structures featuring internal resonance”. In: *Nonlinear Dynamics* Vol. 105.No. 2 (2021), pp. 1237–1272.

[13] Shobhit Jain and George Haller. “How to compute invariant manifolds and their reduced dynamics in high-dimensional finite element models”. In: *Nonlinear dynamics* Vol. 107.No. 2 (2022), pp. 1417–1450.

[14] Andrea Opreni, Alessandra Vizzaccaro, Cyril Touzé, and Attilio Frangi. “High-order direct parametrisation of invariant manifolds for model order reduction of finite element structures: application to generic forcing terms and parametrically excited systems”. In: *Nonlinear Dynamics* Vol. 111.No. 6 (2023), pp. 5401–5447.

[15] Mingwu Li, Shobhit Jain, and George Haller. “Model reduction for constrained mechanical systems via spectral submanifolds”. In: *Nonlinear Dynamics* Vol. 111.No. 10 (2023), pp. 8881–8911.

[16] Adrien Martin, Andrea Opreni, Alessandra Vizzaccaro, Marielle Debeurre, Loic Salles, Attilio Frangi, Olivier Thomas, and Cyril Touzé. “Reduced-order modeling of geometrically nonlinear rotating structures using the direct parametrisation of invariant manifolds”. In: *Journal of Theoretical, Computational and Applied Mechanics* (2023).

[17] Joar Axås and George Haller. “Model reduction for nonlinearizable dynamics via delay-embedded spectral submanifolds”. In: *Nonlinear Dynamics* Vol. 111.No. 24 (2023), pp. 22079–22099.

[18] George Haller, Bálint Kaszás, Aihui Liu, and Joar Axås. “Nonlinear model reduction to fractional and mixed-mode spectral submanifolds”. In: *Chaos: An Interdisciplinary Journal of Nonlinear Science* Vol. 33.No. 6 (2023).

[19] Thomas Thurnher, George Haller, and Shobhit Jain. “Nonautonomous spectral submanifolds for model reduction of nonlinear mechanical systems under parametric resonance”. In: *Chaos: An Interdisciplinary Journal of Nonlinear Science* Vol. 34.No. 7 (2024).
[20] Mingwu Li, Shobhit Jain, and George Haller. “Fast computation and characterization of forced response surfaces via spectral submanifolds and parameter continuation”. In: *Nonlinear Dynamics* (2024), pp. 1–27.
[21] George Haller and Roshan S. Kaundinya. “Nonlinear model reduction to temporally aperiodic spectral submanifolds”. In: *Chaos: An Interdisciplinary Journal of Nonlinear Science* Vol. 34.No. 4 (2024).
[22] Mattia Cenedese, Jacopo Marconi, George Haller, and Shobhit Jain. “Data-assisted non-intrusive model reduction for forced nonlinear finite elements models”. In: *arXiv preprint arXiv:2311.17865* (2023).
[23] Alessandra Vizzaccaro, Giorgio Gobat, Attilio Frangi, and Cyril Touzé. “Direct parametrisation of invariant manifolds for non-autonomous forced systems including superharmonic resonances”. In: *Nonlinear Dynamics* Vol. 112.No. 8 (2024), pp. 6255–6290.
[24] Leonardo Bettini, Mattia Cenedese, and George Haller. “Model reduction to spectral submanifolds in piecewise smooth dynamical systems”. In: *International Journal of Non-Linear Mechanics* Vol. 163 (2024), p. 104753.
[25] Aurélien Grolet, Alessandra Vizzaccaro, Marielle Debeurre, and Olivier Thomas. “High order invariant manifold model reduction for systems with non-polynomial non-linearities: geometrically exact finite element structures and validity limit”. In: (2024).
[26] Malte Krack and Johann Gross. *Harmonic balance for nonlinear vibration problems*. Vol. 1. Springer, 2019.
[27] Carl De Boor and Blâir Swartz. “Collocation at Gaussian points”. In: *SIAM Journal on numerical analysis* Vol. 10.No. 4 (1973), pp. 582–606.
[28] Ehsan Loghman, Ali Kamali, Firooz Bakhtiari-Nejad, Mostafa Abbaszadeh, and Marco Amabili. “On the combined Shooting-Pseudo-Arclength method for finding frequency response of nonlinear fractional-order differential equations”. In: *Journal of Sound and Vibration* Vol. 516 (2022), p. 116521.
[29] Annick Dhooge, Willy Govaerts, and Yu A Kuznetsov. “MATCONT: a MATLAB package for numerical bifurcation analysis of ODEs”. In: *ACM Transactions on Mathematical Software (TOMS)* Vol. 29.No. 2 (2003), pp. 141–164.
[30] A. Vizzaccaro, A. Opreni, L. Salles, and et al. “High order direct parametrisation of invariant manifolds for model order reduction of finite element structures: application to large amplitude vibrations and uncovering of a folding point”. In: *Nonlinear Dynamics* Vol. 110 (2022), pp. 525–571.
[31] Lukas Woiwode, Nidish Narayanaa Balaji, Jonas Kappauf, Fabia Tubita, Louis Guillot, Christophe Vergez, Bruno Cochelin, Aurélien Grolet, and Malte Krack. “Comparison of two algorithms for harmonic balance and path continuation”. In: *Mechanical Systems and Signal Processing* Vol. 136 (2020), p. 106503.
[32] COMSOL AB. *AC/DC Module User’s Guide*. COMSOL Multiphysics®v. 6.2. Stockholm, Sweden, 2023, pp. 75–84.